RSC Advances

ROYAL SOCIETY OF CHEMISTRY

www.rsc.org/advances

Journal Name

ARTICLE

Preparation and microwave absorption properties of uniform TiO_2@C core-shell nanocrystals

Received 00th January 20xx,
Accepted 00th January 20xx

DOI: 10.1039/x0xx00000x

www.rsc.org/

Gengping Wan[a], Lei Yu[a], Xiange Peng[a], Guizhen Wang*[a], Xianqin Huang[a], Haonan Zhao[a] and Yong Qin*[b]

In this work, carbon-coated TiO_2 (TiO_2@C) core-shell nanocrystal has been synthesized by a simple acetylene decomposition method and is further explored for the microwave absorbing application. Results demonstrate that a well-graphitized carbon layer with the thickness of about 3.5 nm can be uniformly coated on the surface of TiO_2. It is found that the microwave absorption properties of TiO_2@C are remarkably enhanced compared to the bare TiO_2. The optimal RL calculated from the measured complex permittivity and permeability is −58.2 dB at 7.6 GHz for TiO_2@C with a loading of 40 wt%. Whereas for TiO_2@C with a loading of 60 wt%, the effective bandwidth of less than −10 dB is found to reach 5.0 GHz with the coating thickness of 2.2 mm. The enhanced performance can be attributed to the increased dielectric properties and the multiple relaxation processes caused by the core–shell composite materials.

Introduction

Electromagnetic (EM) interference problems from the wide application of communication devices have led to the significant interest in developing the high-performance microwave absorption material (MAM) with strong absorption and broad bandwidth.[1-4] Up to now, some possible candidates including magnetic metals,[5,6] carbonaceous materials,[7-10] ferrites,[11,12] ceramics,[13] conducting polymers[14-17] and intermetallic compounds[18] with advanced EM properties have been utilized as fillers into matrices to fabricate MAMs. Despite the good EM performance in some cases, their drawbacks, such as poor stability, high costs and complex synthesis methods have severely impeded their practical applications. Thus it is quite necessary to develop some new MAMs with low cost, easy preparation and good stability.

Titanium dioxide (TiO_2) is one of the most technologically important types of compounds on our planet and has been widely used in many emerging areas including optoelectronics, photovoltaics, catalysis, fuel cells, batteries, smart windows, and self-cleaning and antifogging surfaces, in addition to traditional applications in pigments, UV sunscreens, cosmetics, medical implants, and sensors.[19,20] However, very few reports are available to employ TiO_2 as the MAM due to its poor response in the microwave region. Chen et al showed that hydrogenation of TiO_2 nanocrystals could induce the excellent microwave absorption performance due to the collective movements of interfacial dipoles on the nanometer scale, which opens up new concepts for MAM innovations and inspires further developments of other exciting MAMs.[21,22] In addition, it has been reported that many composite materials with core–shell structures show better microwave absorption properties due to the additional interfacial dielectric relaxation than the pure core or shell materials.[23-29] For example, Shao et al.[30] synthesized core–shell microspheres composed of Ni cores and two phases of TiO_2 (anatase, rutile) shells. In comparison with bare Ni, the composites show better microwave absorption properties. Che and co-workers[31] fabricated the yolk–shell structured Fe_3O_4/TiO_2 composites with enhanced electromagnetic wave absorption. The enhanced electromagnetic absorption of composites is attributed to the unique yolk–shell structure with a large surface area and high porosity, as well as synergistic effects between the functional Fe_3O_4 cores and TiO_2 shells. Based on these considerations, coating TiO_2 with an appropriate EM material using a simple and scalable fabrication technique is considered to be an effective method to improve the microwave absorption performance of TiO_2.

Carbon-based materials have grabbed considerable attention among the EM absorption application because of their outstanding physical properties, including high electrical conductivity, low density, and good stability.[32,33] More recently, it has been confirmed that carbon-coated nanomaterials can also be used as a major annexing agent of microwave absorbers because of their special core–shell structures.[34,35]

In this study, we report a facile and efficient strategy for the synthesis of uniform carbon-coated TiO_2 (TiO_2@C) core-shell nanocrystals and investigate their microwave absorption

[a]Key Laboratory of Tropical Biological Resources of Ministry of Education, Hainan University, Haikou 570228, China
[b]State Key Laboratory of Coal Conversion, Institute of Coal Chemistry, Chinese Academy of Sciences, Taiyuan 030001, China.
Electronic Supplementary Information (ESI) available: [TGA, FTIR, TEM, UV-vis, complex permeability and Attenuation constant]. See DOI: 10.1039/x0xx00000x

properties. Benefiting from the uniform coatings of carbon layers, the interfacial polarization and dielectric properties of TiO_2@C are greatly enhanced, which leads to remarkably improved microwave absorption properties compared to the pristine TiO_2.

Experimental

Preparation

TiO_2 used to prepare TiO_2@C samples was obtained from Degussa (P25 TiO_2). In a typical synthesis, TiO_2 (1.0 g) was introduced into the porcelain boat and transferred to a tube furnace and placed at the centre of the furnace (a quartz tube, 60 mm in diameter and 1100 mm in length), and then a stream of acetylene (an atmosphere pressure) was introduced after evacuation. The temperature was raised at a heating rate of 10 ºC min^{-1}, and the growth of TiO_2@C was performed at 500 ºC for 30 min at atmospheric pressure. After the apparatus was cooled to room temperature, the as-prepared samples were obtained. The growth process of the TiO_2@C core–shell composites is illustrated in Scheme 1.

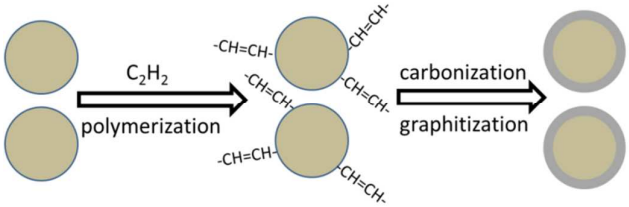

Scheme 1. The growth process of TiO_2@C core-shell composites.

Characterization

The X-ray diffraction (XRD) patterns were collected on a Bruker D8 Advance X-ray diffractometer with Cu *Kα* radiation (λ = 1.54178 Å) using a 40 kV operation voltage and 40 mA current. The TEM and HRTEM images were taken on a JEOL JEM-2100 microscope instrument at an acceleration voltage of 200 kV. Fourier transform infrared spectroscopy (FTIR) spectra were collected on a Bruker TENSOR27 spectrometer, and the sample was prepressed with KBr into pellets before measurement. Thermogravimetric (TG) results were obtained by a thermal analysis system (Q600, TA, America) using ca. 5.0 mg of samples and a heating rate of 10 ºC min^{-1} in air. Raman spectroscopy was performed on a Renishaw inVia Reflex Raman microscope using 532 nm green laser excitation. UV-vis diffuse reflectance spectra (DRS) were measured using PE Lambda 750s UV-Vis spectrophotometer. The specimens for measuring the EM properties were prepared by uniformly mixing desired amount of TiO_2 or TiO_2@C with paraffin and pressing the mixture into a cylindrical shape. Then the cylinder was cut into a toroid of 7.00 mm outer diameter and 3.04 mm inner diameter for measurement. The relative permeability and permittivity values of the mixture were determined and obtained by measuring the S_{11} and S_{21} parameters between 2 and 18 GHz with an AV3629D network analyser by using the transmission/reflection coaxial line method.

Results and discussion

We performed XRD analysis to investigate the crystal phases of the as-prepared products. Fig. 1 shows the XRD patterns of TiO_2 and TiO_2@C products. It is known that the normal phase transition from anatase to rutile TiO_2 nanocrystals requires annealing at around 600 ºC.[36] Moreover, the presence of carbon on the surface of the titania also inhibits its phase transformation, leading to a higher thermal stability.[37] Therefore, it can be found that TiO_2@C is composed of a mixture of anatase and a small number of rutile TiO_2, which are similar to the crystal composition as P25 TiO_2. No clear diffraction peaks of carbon were found for TiO_2@C, which is due to the low content (20.5 wt%) of carbon in the composites confirmed by thermal gravimetric analysis (TGA) experiments (Fig. S1). The FTIR spectra (Fig. S2) reveal that the OH content of TiO_2@C is slightly higher than the bare TiO_2 nanocrystals.

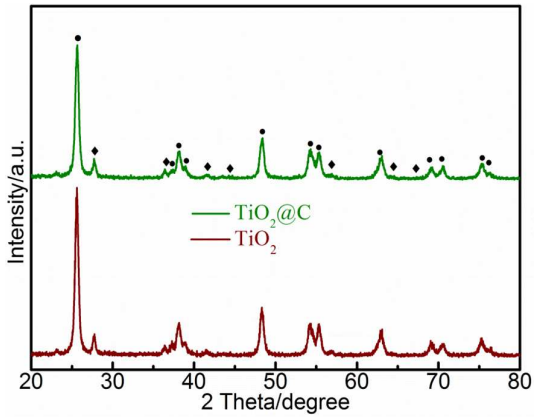

Fig. 1 XRD patterns of TiO_2 and TiO_2@C products.

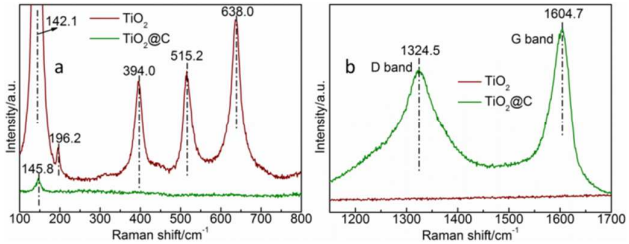

Fig. 2 Raman spectra of TiO_2 and TiO_2@C products: (a) 100–800 cm^{-1}, (b) 1150–1700 cm^{-1}.

We also employed Raman spectroscopy to further characterize the surface functionalities of TiO_2 and TiO_2@C samples qualitatively. In terms of the symmetry group analysis, the characteristic peaks at 143 cm^{-1}, 447 cm^{-1}, 612 cm^{-1}, and 826 cm^{-1} can be ascribed to the B_{1g}, E_g, A_{1g} and B_{2g} Raman active modes of rutile, respectively.[38] Meanwhile, the modes A_{1g} (519 cm^{-1}), B_{1g} (399 and 519 cm^{-1}), and E_g (144, 197, and 639 cm^{-1}) are the Raman-active modes of anatase.[39] Fig. 2a shows the Raman spectra of TiO_2@C nanoparticles by comparison to that of pure P25 TiO_2. The strong characteristic peaks observed in the Raman spectrum of the bare TiO_2 are similar to those of bulk anatase but with a slight shift. For TiO_2@C, only a very weak peak at 145.8 cm^{-1} (E_g) is observed, indicating that a thin layer of carbon possibly exists on the surface of the TiO_2 nanocrystals, as Raman is more sensitive to the sample

surface. The carbon present in the TiO_2@C samples was also investigated by Raman spectroscopy. As shown in Fig. 2b, in the range between 1150 and 1700 cm^{-1}, two strong peaks at 1324.5 and 1604.7 cm^{-1} correspond to the presence of sp^3 defects of carbon (D-band) and the characteristic for graphitic sheets (G-band), respectively. It can be found that the G band peaks of the present TiO_2@C shifted to higher wavelength numbers in comparison with that of well crystalline graphite materials (1575 cm^{-1}), which suggests that the carbon shell is of highly disorderly.[37, 40, 41]

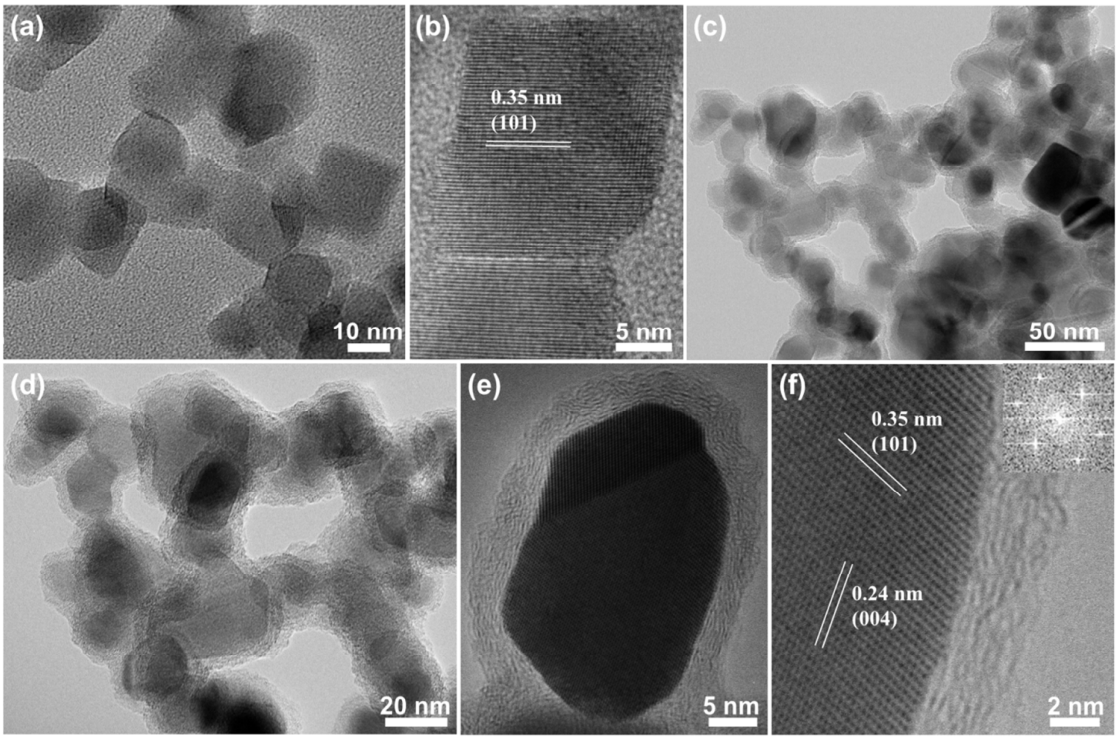

Fig. 3 (a) TEM and (b) HRTEM images of TiO_2. (c–e) TEM images of TiO_2@C. (f) HRTEM image of TiO_2@C.

To further confirm the formation of a carbon layer on the surface of TiO_2 nanocrystals, we performed TEM characterization on TiO_2 and TiO_2@C (Fig. 3). Fig. 3a displays that the bare TiO_2 nanocrystals have an average size in the range of 15–30 nm in diameter. The HRTEM image shows the clear lattice fringes of 0.35 nm corresponding to (101) plane of anatase TiO_2, suggesting the highly crystalline nature of the nanocrystals (Fig. 3b). After a heating process in C_2H_2, the low resolution TEM images show that the TiO_2 particles are surrounded by uniform carbon shells (Fig. 3(c, d)). The formed TiO_2@C core–shell structures are clearly visible due to their different contrasts. Fig 3e displays a HRTEM image of an individual particle. It can be clearly seen that the crystalline TiO_2 particle is coated with a disorderly graphitized carbon layer of about 3.5 nm in thickness. The well-defined crystalline lattice spacing of 0.35 and 0.24 nm from core can be indexed as (101) and (004) crystal planes of anatase TiO_2, respectively. The lattice fringes of the graphitic layers are 0.34 nm, which is in agreement with the previous reports. As can be seen from the HRTEM image (Fig. 3f), there are still some defects within the graphite layers, which is in good agreement with the Raman results. Actually, we also investigated the influence of growth temperature and time on the structures of products (Fig. S3, Fig. S4). But the present method is difficult to efficiently adjust the thickness of carbon shells.

Microwave absorption properties were investigated by mixing 40 wt% and 60 wt% of the samples with paraffin. The reflection loss (RL) curves of TiO_2–paraffin and TiO_2@C–paraffin were derived from the relative complex permittivity and permeability at a given frequency and layer thickness according to the transmit line theory, which can be expressed by the following equations (eqn (1) and (2)):[42-44]

$$Z_{in} = Z_0(\mu_r/\varepsilon_r)^{1/2}\tanh[j(2\pi fd/c)(\mu_r\varepsilon_r)^{1/2}] \quad (1)$$

$$\mathrm{RL} = 20\log\left|(Z_{in} - Z_0)/(Z_{in} + Z_0)\right| \quad (2)$$

where Z_{in} is the input impedance of the absorber, Z_0 the impedance of free space, μ_r the relative complex permeability, ε_r the complex permittivity, f the frequency of microwaves, d the thickness of the absorber, and c the velocity of light. A RL value of −10 dB is comparable to 90% microwave absorption. In general, materials with RL values of less than −10 dB absorption are considered as suitable EM wave absorbers.

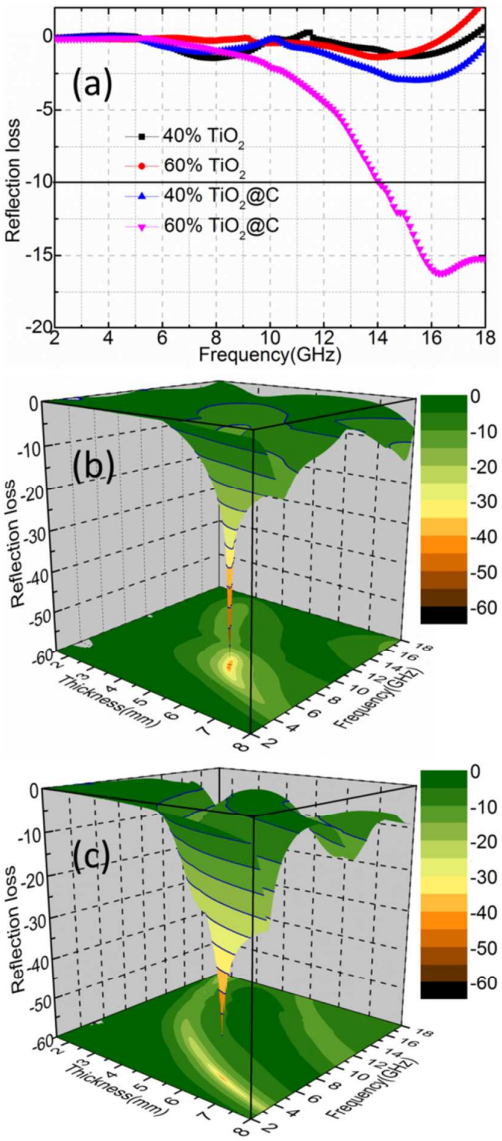

Fig. 4 (a) RL curves of the product/paraffin composites with a thickness of 2.0 mm in the frequency range of 2–18 GHz. Three dimensional representations of RL for TiO_2@C composite absorbers with the loading of (b) 40 wt% and (c) 60 wt%.

Fig. 4a shows a comparison of calculated RL curves in the frequency range of 2−18 GHz for the product/paraffin composites with a thickness of 2 mm. It can be seen that the values of minimum RL of TiO_2 with the loading of 40 wt% and 60 wt% are −1.45 dB and −2.50 dB, while the TiO_2@C with the same appending proportion shows the minimum RL values of −2.98 dB and −16.2 dB, respectively. The microwave absorption value of less than –10 dB for 60 wt% TiO_2@C is in the range of 14.0–18.0 GHz corresponding to a bandwidth of 4.0 GHz. To reveal in detail the influence of thickness on the absorption properties, three-dimensional RL values of TiO_2@C with the loading of 40 wt% and 60 wt% are shown in Fig.4 (b, c). The RL of TiO_2 with the loading of both 40 wt% and 60 wt% almost cannot reach −10 dB which means 90% microwave absorption in the range of 1.5−8.0 mm (not shown). This indicates that the absorption ability of bare TiO_2 is relatively weak. For TiO_2@C with a loading of 40 wt%, a minimum RL value of −58.2 dB at 7.6 GHz and effective bandwidth of 4.26 GHz is obtained with a thickness of 5.5 mm. Whereas for TiO_2@C with a loading of 60 wt%, the effective bandwidth 5.0 GHz is observed with the coating thickness of 2.2 mm, almost covering the whole *Ku*-band (12–18 GHz). Compared with the core-shell structured absorption materials reported recently,[27,29,44–46] the present TiO_2@C also has a broader bandwidth with a smaller coating thickness. Moreover, the absorption band for RL values below −10 dB almost covers the whole frequency range with a thickness of 1.5−8 mm, which demonstrates that the EM wave absorption frequency band can be tuned by properly selecting the coating thickness. The above results reveal that TiO_2 coated by carbon film is a very efficient way for the improvement of the EM absorption properties.

In order to uncover how the TiO_2@C core-shell nanostructures affect the absorption properties of composites, the relative complex permittivity ($\varepsilon_r = \varepsilon' + i\varepsilon''$) and permeability ($\mu_r = \mu' + i\mu''$) were evaluated at 2–18 GHz. It is well known that the real parts of complex permittivity (ε') and permeability (μ') represent the storage ability of electric and magnetic energy, and the imaginary parts (ε'' and μ'') are related to the dissipation (or loss) capability. Owing to the absence of magnetic constituents in the composites, the real (μ') and imaginary (μ'') parts of the complex permeability are about 1.0 and 0.0, respectively (Fig. S5). The measured complex permittivity spectra of the TiO_2-paraffin and TiO_2@C-paraffin composites are shown in Fig. 5. It can be seen that TiO_2-paraffin composites with the loading of 40 wt% have a relatively stable ε' value of 2.9–3.4 in the frequency range of 2–18 GHz, while the TiO_2@C-paraffin composites with the loading of 40 wt% display a much higher ε' value (Fig. 5a). The ε' value decreases gradually from 5.3 at 2.0 GHz to 3.6 at 9.3 GHz, then increases to 3.7 at 10.9 GHz, and decreases to 3.2 at 18.0 GHz. It can be seen in Fig. 5b that TiO_2@C has much higher ε'' value than that of pure TiO_2 in the frequency range of 2–18 GHz. The ε'' value is in the range of 0.4–2.6, which is about 7 times higher than that of the bare TiO_2. Furthermore, as shown in Fig. 5(c, d), TiO_2-paraffin composites show a slightly improved ε' value of 3.8–4.4 and a relatively small ε'' value (less than 0.15) when the loading of composites is increased to 60 wt%. Correspondingly, TiO_2@C-paraffin composites display significantly increased ε' and ε'' values from 7.9 to 4.5 and from 1.8 to 5.3, respectively. The higher ε' and ε'' values indicate that TiO_2@C has much higher efficiency in storing and dissipating the electrical energy.

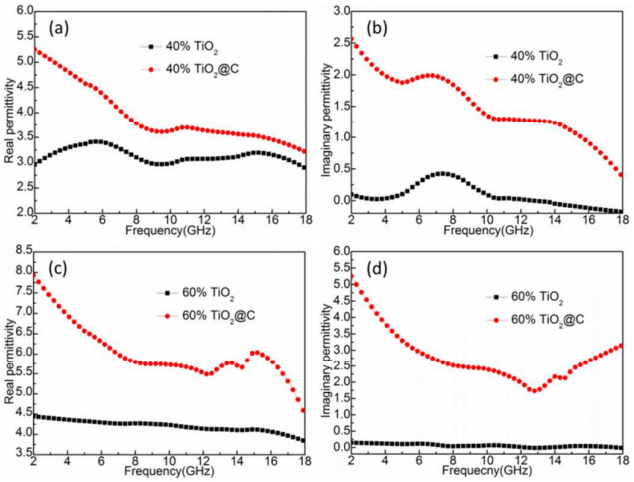

Fig. 5 The frequency dependence of real and imaginary permittivity of the product/paraffin composites with the loading of (a, b) 40 wt% and (c, d) 60 wt%.

We calculated the dielectric loss tangent (tan $\delta_E = \varepsilon''/\varepsilon'$) of TiO_2-paraffin and TiO_2@C-paraffin composites with different loadings (Fig. 6). The dielectric losses of TiO_2-paraffin with the loading of both 40 wt% and 60 wt% are no higher than 0.15 in the whole frequency range from 2 to 18 GHz. For the TiO_2@C-paraffin composites, the maximum values of tan δ_E are 0.49 and 0.70 corresponding to the loading of 40 wt% and 60 wt%, respectively. The relatively high values of tan δ_E imply that the TiO_2@C exhibits more intense dielectric loss. Moreover, the increasing loading of TiO_2@C leads to an improvement of the dielectric loss. Generally, the high dielectric loss is useful for improving the attenuation constant α which determines the attenuation properties of materials. In Fig. S6, it can be seen that the TiO_2@C-paraffin composites have larger α value at 2–18 GHz. Therefore, the TiO_2@C core-shell nanocrystals exhibit better EM-absorption properties than the bare TiO_2 over the whole frequency range.

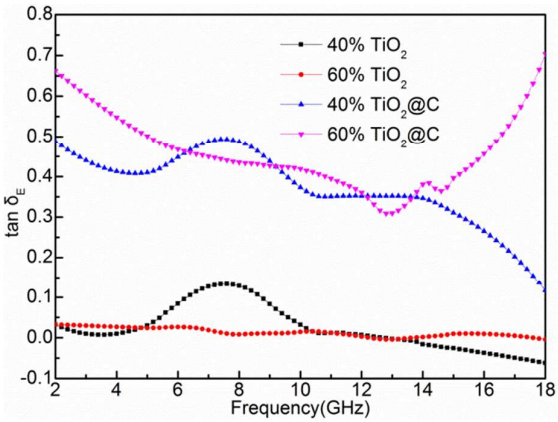

Fig. 6 The frequency dependence of dielectric loss tangents of the TiO_2–paraffin composite and TiO_2@C–paraffin composite.

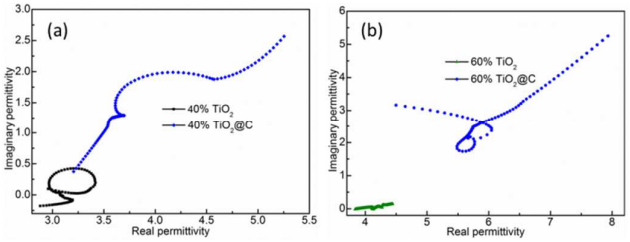

Fig. 7 Typical Cole–Cole semicircles (ε'' versus ε') for TiO_2–paraffin composite and TiO_2@C–paraffin composite in the frequency range of 2–18 GHz.

The Debye dipolar relaxation can be utilized to understand permittivity behaviours of microwave absorption materials. Fig. 7 shows ε'–ε'' curves of TiO_2 and TiO_2@C composites in the frequency range of 2–18 GHz. It is evident that TiO_2 presents just one small Cole–Cole semicircle, implying that there is a weak dielectric relaxation process. Three Cole–Cole semicircles are found for the TiO_2@C composites, which may indicate that there are multiple dielectric relaxation processes. It also demonstrates that the carbon shell on the surface of TiO_2 is helpful for increasing the intensity of the Debye dipolar relaxation process.

Interfacial polarization occurs whenever there is a build-up of a charge at a boundary between two regions or materials.[21] In our case, benefiting from the excellent conductivity of carbon shell, the charge transfer between TiO_2 and carbon also occurs with little hindrance. Therefore, the existence of interfaces between TiO_2–TiO_2, carbon–carbon and TiO_2–carbon may give rise to the interfacial polarization and the associated relaxation, which should contribute to the enhanced dielectric loss and microwave absorption performance. To further give a visual demonstration of the microwave absorption mechanism of TiO_2@C composites as discussed above, a schematic is given in Scheme 2.

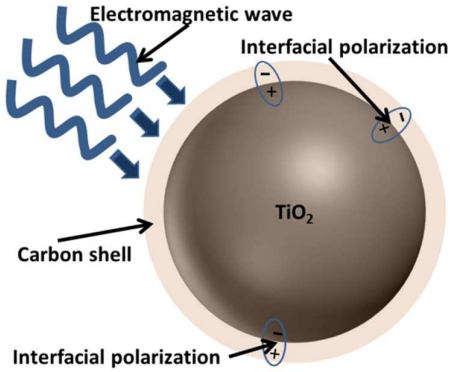

Scheme 2. Schematic representation of the interfacial-polarization-improved microwave absorption mechanism for the TiO_2@C.

The optical properties of the TiO_2@C samples were probed with UV-vis diffuse reflectance spectroscopy (Fig. S7). Compared with the pure TiO_2 nanoparticles, the carbon-coated samples show enhanced visible-light absorption. In addition, based on the fact that the improved electronic conductivity can be obtained by

uniformly coated carbon shell, it can be believed that the present TiO_2@C with the perfect core-shell structure can not only be used to absorb EM wave, but also be extended to other application areas, such as photocatalysis and lithium ion batteries.

Conclusions

TiO_2@C nanocrystals are successfully fabricated through an acetylene decomposition method. The products exhibit excellent microwave absorption performance, which results from the increased complex permittivity and the multiple relaxation processes. The present TiO_2@C core-shell nanocrystals can be used as a new type of broadband microwave absorbent, and probably have important application in photocatalysis and lithium ion battery fields.

Acknowledgements

This work was supported by the National Natural Science Foundation of China (11564011, 51362010), the Natural Science Foundation of Hainan Province (514207, 514212), the Scientific Research Projects of Colleges and Universities of Hainan Province (HNKY2014-14), and the Scientific Research Projects of Hainan University (kyqd1502).

Notes and references

1 H. Sun, R. Che, X. You, Y. Jiang, Z. Yang, J. Deng, L. Qiu and H. Peng, *Adv. Mater.*, 2014, **26**, 8120.
2 L. Kong, Z. Li, L. Liu, R. Huang, M. Abshinova, Z. Yang, C. Tang, P. Tan, C. Deng and S. Matitsine, *Int. Mater. Rev.*, 2013, **58**, 203.
3 G. Wang, X. Peng, L. Yu, G. Wan, S. Lin and Y. Qin, *J. Mater. Chem. A*, 2015, **3**, 2734.
4 M.-S. Cao, X.-X. Wang, W.-Q. Cao and J. Yuan, *J. Mater. Chem. C*, 2015, **3**, 6589.
5 X. Zhang, P. Guan and X. Dong, *Appl. Phys. Lett.*, 2010, **97**, 033107.
6 C. Wang, X. Han, P. Xu, J. Wang, Y. Du, X. Wang, W. Qin and T. Zhang, *J. Mater. Chem. C*, 2010, **114**, 3196.
7 B. Wen, M. Cao, M. Lu, W. Cao, H. Shi, J. Liu, X. Wang, H. Jin, X. Fang, W. Wang and J. Yuan, *Adv. Mater.*, 2014, **26**, 3484.
8 G. Wang, Z. Gao, S. Tang, C. Chen, F. Duan, S. Zhao, S. Lin, Y. Feng, L. Zhou and Y. Qin, *ACS Nano*, 2012, **6**, 11009.
9 Y. Zhang, Y. Huang, T. Zhang, H. Chang, P. Xiao, H. Chen, Z. Huang and Y. Chen, *Adv. Mater.*, 2015, **27**, 2049.
10 G. Wang, Z. Gao, G. Wan, S. Lin, P. Yang and Y. Qin, *Nano Research*, 2014, **7**, 704.
11 G. Sun, B. Dong, M. Cao, B. Wei and C. Hu, *Chem. Mater.*, 2011, **23**, 1587.
12 J. Liu, R. Che, H. Chen, F. Zhang, F. Xia, Q. Wu and M. Wang, *Small*, 2012, **8**, 1214.
13 F. Xia, J. Liu, D. Gu, P. Zhao, J. Zhang and R. Che, *Nanoscale*, 2011, **3**, 3860.
14 K. Lakshmi, H. John, K. Mathew, R. Joseph and K. George, *Acta Mater.*, 2009, **57**, 371.
15 G.-S. Wang, X.-J. Zhang, Y.-Z. Wei, S. He, L. Guo and M.-S. Cao, *J. Mater. Chem. A*, 2013, **1**, 7031.
16 Y.-Z. Wei, G.-S. Wang, Y. Wu, Y.-H. Yue, J.-T. Wu, C. Lu and L. Guo, *J. Mater. Chem. A*, 2014, **2**, 5516.
17 X.-J. Zhang, G.-S. Wang, Y.-Z. Wei, L. Guo and M.-S. Cao, *J. Mater. Chem. A*, 2013, **1**, 12115.
18 N.-N. Song, Y.-J. Ke, H.-T. Yang, H. Zhang, X.-Q. Zhang, B.-G. Shen and Z.-H. Cheng, *Sci. Rep.*, 2013, **3**, 2291.
19 M. Cargnello, T. R. Gordon and C. B. Murray, *Chem. Rev.*, 2014, **114**, 9319.
20 H. Zhang and J. F. Banfield, *Chem. Rev.*, 2014, **114**, 9613.
21 T. Xia, C. Zhang, N. A. Oyler and X. Chen, *Adv. Mater.*, 2013, **25**, 6905.
22 T. Xia, C. Zhang, N. A. Oyler and X. Chen, *J. Mater. Res.*, 2014, **29**, 2198.
23 B. Zhao, G. Shao, B. Fan, W. Zhao, Y. Xie and R. Zhang, *RSC Adv.*, 2014 **4**, 61219.
24 K. Yuan, R. Che, Q. Cao, Z. Sun, Q. Yue and Y. Deng, *ACS Appl. Mat. Interfaces*, 2015, **7**, 5312.
25 X. Liu, D. Geng, H. Meng, P. Shang and Z. Zhang, *Appl. Phys. Lett.*, 2008, **92**, 173117.
26 X. Liu, B. Li, D. Geng, W. Cui, F. Yang, Z. Xie, D. Kang and Z. Zhang, *Carbon*, 2009, **47**, 470.
27 Y. Zhu, Q. Ni and Y. Fu, *RSC Adv.*, 2015, **5**, 3748.
28 M. Yu, C. Liang, M. Liu, X. Liu, K. Yuan, H. Cao and R. Che, *J. Mater. Chem. C*, 2014, **2**, 7275.
29 B. Zhao, G. Shao, B. Fan, Y. Chen and R. Zhang, *Physica B*, 2014, **454**, 120.
30 B. Zhao, G. Shao, B. Fan, W. Zhao, Y. Xie and R. Zhang, *Phys. Chem. Chem. Phys.*, 2015, **17**, 8802.
31 J. Liu, J. Xu, R. Che, H. Chen, M. Liu and Z. Liu, *Chem.-Eur. J.*, 2013, **19**, 6746.
32 F. Qin and C. Brosseau, *J. Appl. Phys.*, 2012, **111**, 061301.
33 G. Wang, G. Ran, G. Wan, P. Yang, Z. Gao, S. Lin, C. Fu and Y. Qin, *ACS Nano*, 2014, **8**, 5330.
34 Y.-J. Chen, G. Xiao, T.-S. Wang, Q.-Y. Ouyang, L.-H. Qi, Y. Ma, P. Gao, C.-L. Zhu, M.-S. Cao and H.-B. Jin, *J. Mater. Chem. C*, 2011, **115**, 13603.
35 X. Liu, Z. Ou, D. Geng, Z. Han, J. Jiang, W. Liu and Z. Zhang, *Carbon*, 2010, **48**, 891.
36 X. Chen and S. S. Mao, *Chem. Rev.*, 2007, **107**, 2891.
37 L.-W. Zhang, H.-B. Fu and Y.-F. Zhu, *Adv. Funct.*, Mater 2008, **18**, 2180.
38 S. Porto, P. Fleury and T. Damen, *Phys. Rev.*, 1967, **154**, 522.
39 T. Ohsaka, F. Izumi and Y. Fujiki, *J. Raman Spectrosc.* 1978, **7**, 321.
40 F. Tuinstra and J. L. Koenig, *J. Chem. Phys.* 1970, **53**, 1126.
41 L. Zhang, H. Cheng, R. Zong and Y. Zhu, *J. Phys. Chem. C*,2009, **113**, 2368.
42 R. Che, L. M. Peng, X. F. Duan, Q. Chen and X. Liang, *Adv. Mater.*, 2004, **16**, 401.
43 J. Liu, W.-Q. Cao, H.-B. Jin, J. Yuan, D.-Q. Zhang and M.-S. Cao, *J. Mater. Chem. C*, 2015, **3**, 4670.
44 H. Lv, G. Ji, X. Liang, H. Zhang and Y. Du, *J. Mater. Chem. C*, 2015, **3**, 5056.
45 B. Zhao, B. Fan, G. Shao, W. Zhao and R. Zhang, *ACS Appl. Mater. Interfaces*, 2015, **7**, 18815.
46 H. Wang, L. Wu, J. Jiao, J. Zhou, Y. Xu, H. Zhang, Z. Jiang, B. Shen and Z. Wang, *J. Mater. Chem. A*, 2015, **3**, 6517.

TOC

Uniform carbon-coated TiO_2 core-shell nanocrystals are synthesized and can be used as a new type of broadband microwave absorbers.